

INTERACTION OF THE SOLAR WIND WITH THE PLANET MARS: *PHOBOS 2* MAGNETIC FIELD OBSERVATIONS

W. RIEDLER, K. SCHWINGENSCHUH and H. LICHTENEGGER
Institut für Weltraumforschung ÖAW, 8010 Graz, Inffeldgasse 12, Austria

D. MÖHLMANN and J. RUSTENBACH
Institut für Kosmosforschung, Rudower Chaussee 5, 1199 Berlin, G.D.R.

YE. YEROSHENKO
IZMIRAN, Troitsk, Moscow region, U.S.S.R.

J. ACHACHE
Institute de Physique du Globe, Paris, France

J. SLAVIN
GSFC, Greenbelt, MD 20771, U.S.A.

and

J. G. LUHMANN and C. T. RUSSELL
IGPP/UCLA, Los Angeles, CA 90024, U.S.A.

(Received 12 April 1990)

Abstract—The magnetometers on board the *Phobos 2* spacecraft provided the opportunity to study the magnetic environment around Mars, including regions which have never been explored before, such as at low altitudes (down to 850 km above the surface of Mars) and in the tail. The data revealed a bow shock, characterized by a distinct jump in the magnetic field strength and a boundary denoted “planetopause”, where the level of turbulence of the magnetic field changes. Inside the planetopause the field remains quiet.

Some of the main characteristics of the bow shock and the magnetosheath can be reproduced by computer simulations within the framework of a gas-dynamic model using the observed planetopause as an obstacle for the incoming solar wind.

In many spacecraft orbits around Mars, reversals of the B_x -component were found which are typical for tail crossings. A first analysis of the tail data from the circular orbits at a distance of 2.8 Mars radii showed several cases where the reversal of the tail lobes was controlled by the IMF. This supports the idea of an induced character of the solar wind interaction with Mars outside a distance of about 2.8 Mars radii. However, there are certain features in the magnetic field data which could be interpreted as traces of a weak Martian intrinsic field.

INTRODUCTION

Among the terrestrial planets, the solar wind-planet interaction has most intimately been explored at the Earth and at Venus. The Earth, due to its intrinsic magnetic field ($M = 8 \times 10^{25} \text{ G cm}^3$) forms a large obstacle which makes the solar wind be shielded from the surface and to be largely diverted about the planet, leaving a region of about 200,000 km across which is solely dominated by the Earth's magnetic field. During average IMF conditions the subsolar stand-off distance of the terrestrial bow shock is about 13.8 Earth radii (R_E), and the distance in the dawn-dusk plane is about 23.5 R_E (Fairfield, 1971). The average

height of the magnetosphere at the subsolar point is $\approx 10.4 R_E$. At Venus, though similar to Earth in size, the nature of the interaction is quite different. Due to the lack of a significant internal magnetic field ($M \leq 4.3 \pm 2.0 \times 10^{21} \text{ G cm}^3$, Russell *et al.*, 1980), the solar wind plasma directly hits the upper atmosphere/ionosphere thus powering ionospheric currents, their magnetic fields being capable of deflecting the solar wind. Therefore the Venusian “magnetosphere” is inductive in nature and much smaller than that of the Earth, the cross-section being barely larger than the geometrical cross-section of the planet. The average nose and terminator radii of the bow shock are ≈ 1.38 and ≈ 2.38 Venus radii (Russell, 1985). The subsolar

height of the obstacle corresponds to the height of the ionopause, being only insignificantly above the surface.

For Mercury, based on *Mariner 10* data a magnetospheric type of interaction was inferred, leading to an estimate of the dipole moment of $M \approx 2.4 \times 10^{22}$ G cm³ (e.g. Whang, 1977). The subsolar shock radius was found to be 1.9 Mercury radii (R_{Me}), the terminator shock radius is $\approx 3.3 R_{Me}$ and the subsolar radius of the magnetosphere is about 1.3 R_{Me} (Russell, 1985). Although the bow shock of Mercury is much smaller in size than that of the Earth, it is similar in shape.

Little is known about the nature of the solar wind interaction with Mars, even though it has been visited by many spacecraft. The reason is that only four spacecraft, *Mariner 4*, and *Mars 2*, 3 and 5 were properly equipped with instruments to carry out measurements concerning the particle and field environment of Mars. All these missions have clearly detected a bow shock, indicating that the flow is deflected rather than absorbed by the planet. Controversy, however, arose on the exact location of the bow shock, specifically on the nose position. Depending on the presumed nose position and the interpretation of tail data, magnetospheric-like and ionospheric-like interactions have been favored by various authors (e.g. Dolginov *et al.*, 1976; Dolginov, 1978a, b; Russell, 1978a, b; Vaisberg and Smirnov, 1986). Using *Mars 2*, 3 and 5 data, Russell (1977) has found a shock nose radius of 1.5 Mars radii (R_M), a shock terminator radius of 3 R_M and a subsolar obstacle height of 1.1 R_M . The scarcity of our knowledge about the interaction process at Mars is also reflected by the great variety of dipole moments which are offered: they range from $\approx 2 \times 10^{21}$ G cm³ (Russell, 1978) to $\approx 8 \times 10^{22}$ G cm³ (e.g. O'Gallagher and Simpson, 1965).

All former spacecraft which hitherto carried a magnetometer did not come closer than ≈ 1100 km above the Martian surface. Also, no measurements directly behind the planet have been available so far. The trajectory of *Phobos 2* thus allowed for the first time the collection of data in regions which are relevant for the solar wind-Mars interaction investigations and which have not been explored before.

INSTRUMENTATION

The two three-axes fluxgate sensors of the MAGMA and FGMM instruments were mounted on the top of a 3.6 m boom and 1 m closer in, respectively. Both instruments had a dynamic range of ± 100 nT and a sampling rate of 20 vectors s⁻¹ (MAGMA) and

60 vectors s⁻¹ (FGMM). Data were transmitted every 1.5, 2.5, 45 and 600 s, depending on the telemetry mode of the spacecraft. In addition, a spectral analysis was performed on board and transmitted every 30 or 900 s, according to the mode. The accuracy of the magnetometers, defined as the error of the total offset, was about 0.2 nT. A detailed description of the MAGMA instrument can be found in Aydogar *et al.* (1989).

OBSERVATIONS

Upon arrival, *Phobos 2* entered a highly elliptical orbit around Mars with a periaxis of 4250 km and an apoaxis of 84,700 km. After four nearly identical orbits with periods of 77 h the spacecraft was manoeuvred into a circular orbit with a radius of 9600 km and an 8 h period. Figure 1 shows the spacecraft trajectories and the general features of the solar wind interaction with Mars in cylindrical, Mars-centered areo-orbital coordinates; crosses and squares denote observed positions of the bow shock and the planetopause, respectively, and time marks indicate hours before and after closest approach (CA). The bow shock in Fig. 1 best fits the data obtained during the third elliptic orbit and was calculated by means of the gas-dynamic model of Spreiter and Stahara (1980), using the indicated parameters as input and the observed planetopause as the boundary of the obstacle.

Figure 2 gives an overview of the magnetic field measurements along all elliptical orbits. The interaction regions during the encounter phases are clearly distinguished. The magnetosheath passage along orbit 3 (8 February) seems to be more pronounced in the data than that of orbit 1 (1 and 2 February), 2 (4 and 5 February) and 4 (11 February). The undisturbed solar wind magnetic field strength did not exceed ≈ 4.5 γ . During the elliptic orbits the solar wind remains quite steady with a velocity between 400 and 500 km s⁻¹ (Dubinin, private communication). One exception occurred at the encounter of the first orbit when a free stream velocity of about 750 km s⁻¹ was registered.

High resolution magnetic field measurements obtained during the first elliptic orbit near pericenter are shown in Fig. 3. Starting from $\approx 18:10$ U.T., the field magnitude becomes increasingly turbulent, showing a distinct jump at $\approx 18:25$ U.T. at a distance of 4980 km from the center of the planet. This jump has been identified as the bow shock crossing (BS in Fig. 3). Behind the shock, the level of turbulence has increased as is expected within the magnetosheath. At $\approx 18:37$ U.T., 4280 km apart from the center the fluctuations suddenly disappear and the field remains quiet. This characteristic feature has been associated

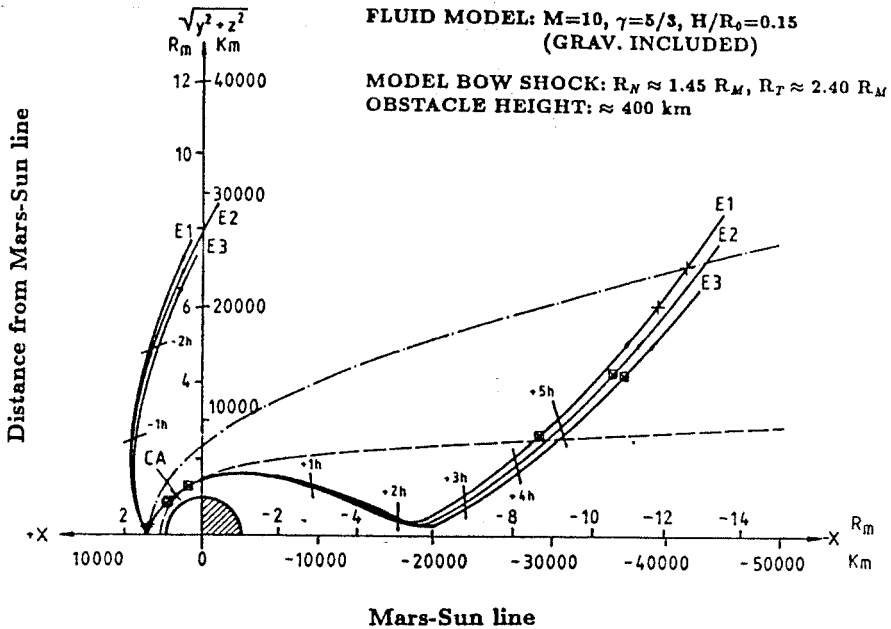


FIG. 1. MAIN BOUNDARIES OBSERVED BY THE MAGMA AND FGMM EXPERIMENTS DURING THE FIRST THREE LOW-ALTITUDE ELLIPTICAL ORBITS (E1, E2, E3) AROUND MARS.

Tick marks indicate hours with respect to closest approach (CA). Crosses and squares denote observed crossings of bow shock and planetopause, respectively. The parameters shown are used in the numerical model, where M is the Mach number, γ is the ratio of specific heats and H/R_0 is the scale height in units of the subsolar obstacle radius. R_N and R_T denote the nose and terminator radius of the bow shock.

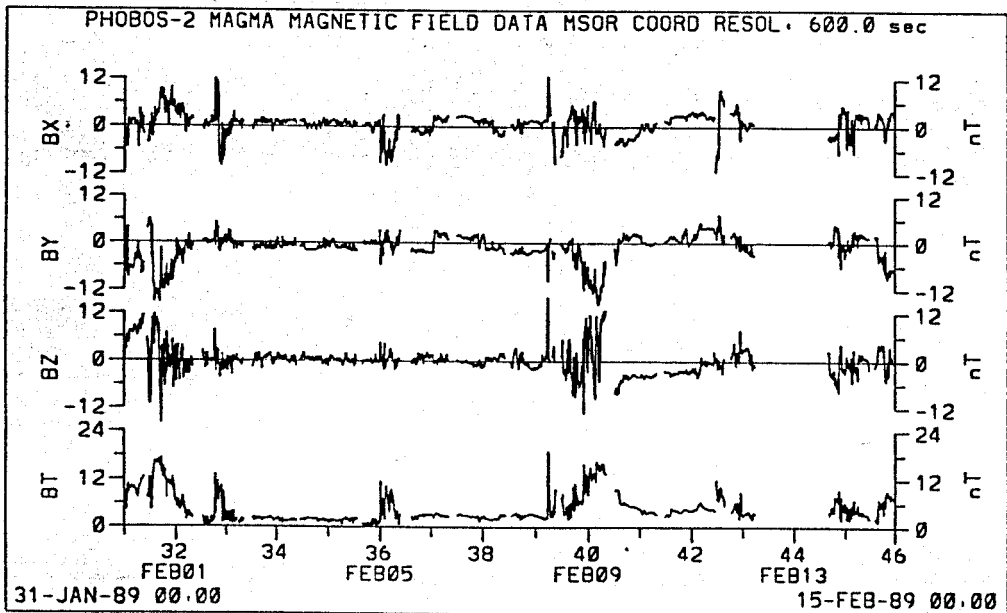


FIG. 2. RESULTS OF MAGNETIC FIELD MEASUREMENTS (B_x , B_y , B_z , B_t in NANOTESLAS FROM THE UPPER TO LOWER PANEL) DURING THE ELLIPTICAL ORBITS AROUND MARS.

The X -axis of the coordinate system points towards the Sun, the y -axis is in the opposite direction to the planetary motion, and the z -axis completes the right-handed system. Time resolution: 600 s.

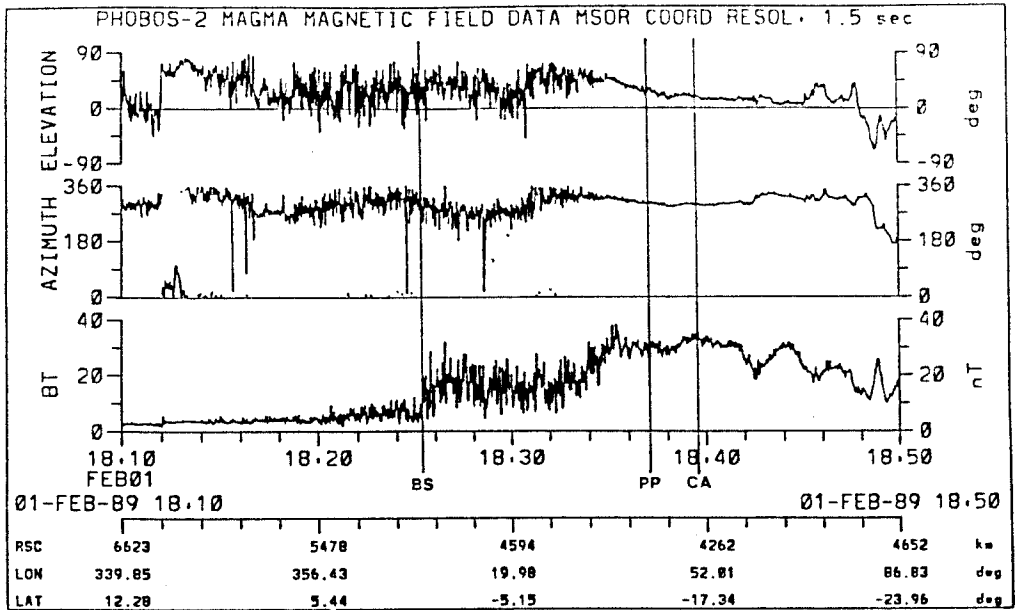


FIG. 3. MAGNITUDE AND ORIENTATION OF MAGNETIC FIELD VECTORS NEAR CLOSEST APPROACH (CA) DURING THE FIRST ELLIPTIC ORBIT.

The azimuth is measured with respect to the x -axis, the elevation with respect to the x, y -plane (see Fig. 2). The lower panel shows the distance of the spacecraft (RSC) from the center of Mars in kilometers as well as its longitude and latitude (LON, LAT) in degrees. BS and PP denote inbound bowshock and inbound planetopause, respectively. Time resolution: 1.5 s.

with a boundary that was called "planetopause" (cf. Riedler *et al.*, 1989). At this boundary there is also a distinct drop in the solar wind proton density (Rosenbauer *et al.*, 1989), strongly suggesting that the planetopause coincides with the outer boundary of the "obstacle". In Fig. 4, which shows the field magnitude for the first three elliptic orbits in the bow shock region, the data have been filtered with a low pass filter, using a corner frequency of 0.01 Hz. The rise of the field in front of the shock (starting in each case about 13 min before the main bow shock crossing) represents the foot of the shock which is associated with reflected ions (see Gosling and Thomsen, 1985), showing a thickness of about 1300–1400 km. Until the premature end of the mission, magnetic field measurements for more than 80 circular orbits were obtained. These orbits allowed measurements directly behind the planet and are thus also well suited for studies of the near Martian tail.

In Fig. 5 the results of the measurements along one of the circular orbits on 16 March 1989 are illustrated. The inbound and outbound crossings of the bow shock characterized by a jump in the total field are well established; the planetopause crossings are somewhat less striking but are often attended by a jump and a

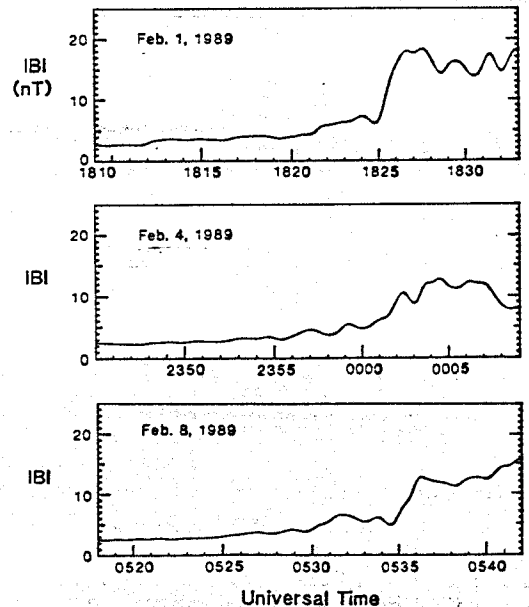


FIG. 4. MAGNETIC FIELD MAGNITUDE NEAR BOW SHOCK CROSSINGS DURING THE FIRST THREE ELLIPTIC ORBITS. The data have been filtered with a low pass filter with a 0.01 Hz corner frequency.

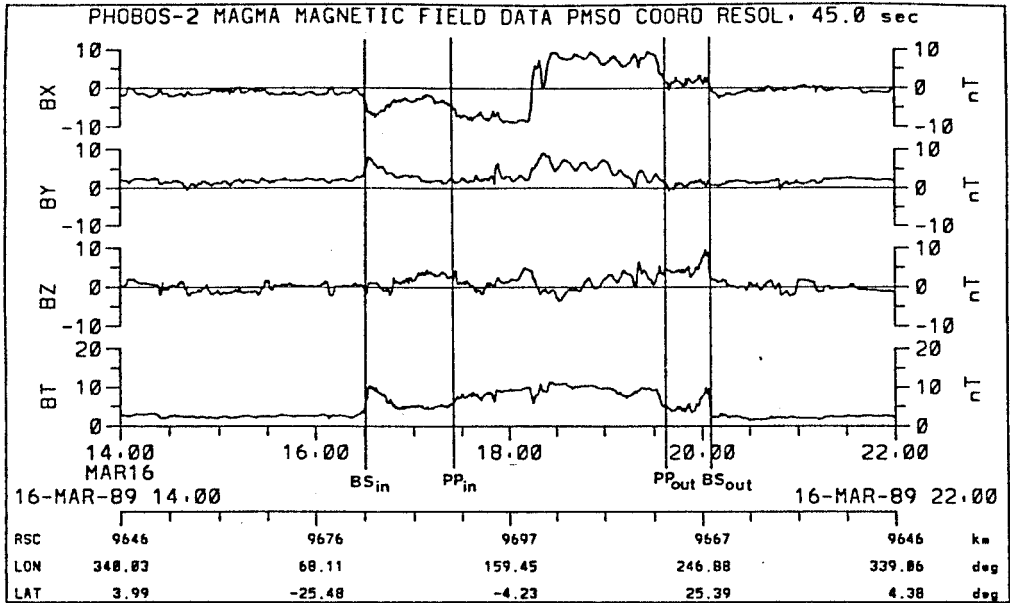


FIG. 5. MAGNITUDE AND COMPONENTS OF THE MAGNETIC FIELD ALONG ONE OF THE CIRCULAR ORBITS ON 16 MARCH 1989.

The coordinate system is the same as in Fig. 2. BS_{in} , PP_{in} , PP_{out} and BS_{out} indicate inbound and outbound crossings of bow shock and planetopause. Time resolution: 45 s.

rotation of the magnetic field. It should be noted, however, that due to the low resolution (1 vector per 45 s) small scale structures cannot be reproduced. The field reversal of B_x at $\approx 18:30$ U.T. can be interpreted as the crossing of the tail, a feature frequently observed in the data.

If the field is draped around the planet one would expect a negative y -component of the undisturbed IMF to cause a $+/-$ reversal of the x -component and vice versa. Indeed, by inspection of Fig. 2 one can verify a $+/-$ polarity of the lobes at the first three orbits corresponding to a negative y -component and an opposite polarity at the fourth orbit, associated with a positive y -component (see also Fig. 5). This polarity change in response to the IMF was also observed during the circular orbits, when a sector boundary (10 March 1989) passed the planet. Thus the polarity of the reversal predominantly depends on the orientation of the upstream IMF, indicating an induced magnetotail at distances outside about 2.8 Mars radii (see Yeroshenko *et al.*, 1991). However, the induced character of the tail does not imply the total absence of any intrinsic field. Based on a period analysis, Möhlmann *et al.* (1991, this issue) have found hints for a corotating part in the measured fields

which could be interpreted in favor of the existence of a weak Martian magnetic field.

The location of the bow shock as observed during the circular orbits appears to be quite variable (see Fig. 6). By comparison of those dawn and dusk crossings of the bow shock that can clearly be identified in the data one can derive an average aberration angle of about 3.2° . This corresponds to an average solar wind velocity of 430 km s^{-1} . Observations during the elliptical orbits and computer simulations both show that the subsolar position of the bow shock is only less affected by reasonable variations of the IMF. Therefore we use the subsolar shock location of $1.45 R_M$ obtained from the first elliptical orbit (which agrees well with the average shock position of $1.47 R_M$ found by Schwingschuh *et al.*, 1991) and combine it with the average shock location near the terminator plane obtained from the circular orbits to find the mean shape of the shock. Assuming a temperature of $1 \times 10^5 \text{ K}$, a number density of 3 cm^{-3} and a magnetic field strength of 3 nT for the undisturbed IMF, the average shock was calculated by means of the Stahara-Spreiter model, using a Mach number of 8 and a ratio of specific heats of $5/3$. The resulting shock is illustrated in Fig. 6 together with the corresponding

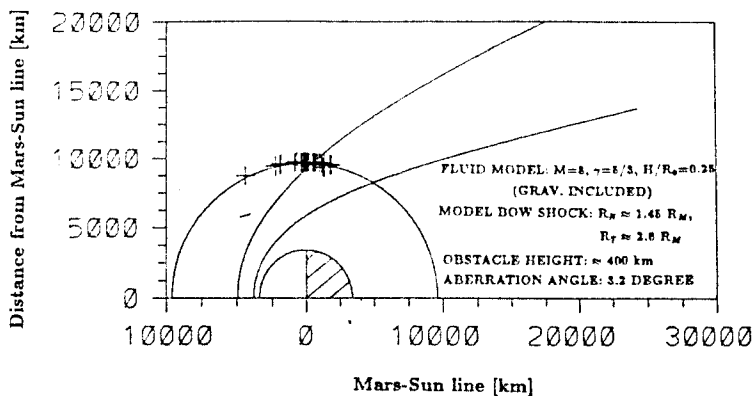


FIG. 6. MEAN BOW SHOCK AND PLANETOPAUSE OBTAINED BY THE NUMERICAL MODEL USING MEASUREMENTS OF THE CIRCULAR ORBITS AND AN AVERAGE ABERRATION ANGLE OF 3.2° . Crosses denote those observed dusk bow shock locations that can clearly be identified. For the coordinate system and the meaning of parameters see Fig. 1.

boundary of the obstacle. As can be seen, in order to fit the average shock position, an obstacle with quite a flaring tail is needed.

CONCLUSIONS

The *Phobos* mission provided data down to 850 km above the dayside surface of Mars and many measurements in the wake at a distance of about 9600 km from the center of Mars. Two distinct boundaries were detected: the bow shock and the planetopause. The latter separates the solar wind dominated region from the region dominated by ions of Martian origin and is also characterized by a drop of magnetic turbulence. Using the observed data together with a computer model we have deduced a subsolar height of the planetopause of about 400 km above the surface and a bow shock stand off distance of approximately $1.45 R_M$.

During the circular orbit phase the location of the shock appeared to be quite variable. Using average solar wind conditions, a mean terminator radius of about $2.6 R_M$ is found.

Finally, the sensitivity of the tail lobes to the IMF direction at a distance of $2.8 R_M$ suggests an induced character of the tail at least outside that distance.

REFERENCES

- Aydogar, Oe., Schwingenschuh, K., Schelch, G., Arnold, H., Berghofer, G. and Riedler, W. (1989) The *Phobos* Fluxgate Magnetometer (MAGMA) Instrument Description. Report IWF-8904 of the Space Research Institute of the Austrian Academy of Sciences.
- Dolginov, Sh. Sh. (1978a) The magnetic field of Mars: *Mars 2* and *Mars 3* evidence. *Geophys. Res. Lett.* **5**, 89.
- Dolginov, Sh. Sh. (1978b) The magnetic field of Mars: *Mars 5* evidence. *Geophys. Res. Lett.* **5**, 93.
- Dolginov, Sh. Sh., Yeroshenko, Ye. G. and Zhuzgov, L. N. (1976) The magnetic field of Mars according to the data from the *Mars 3* and *Mars 5*. *J. geophys. Res.* **81**, 3535.
- Fairfield, D. H. (1971) Average and unusual locations of the Earth's magnetopause and bow shock. *J. geophys. Res.* **76**, 6700.
- O'Gallagher, J. J. and Simpson, J. A. (1965) Search for trapped electrons and a magnetic moment at Mars by *Mariner IV*. *Science* **149**, 1233.
- Gosling, J. T. and Thomsen, M. F. (1985) Specularly reflected ions, shock foot thickness, and shock velocity determinations in space. *J. geophys. Res.* **90**, 9893.
- Möhlmann, D., Riedler, W., Rustenbach, J., Schwingenschuh, K., Kurths, J., Motschmann, U., Roatsch, T., Sauer, K. and Lichtenegger, H. T. M. (1991) The question of an internal Martian magnetic field. *Planet. Space Sci.* **39**, 83.
- Riedler, W., Möhlmann, D., Oraevsky, V. N., Schwingenschuh, K., Yeroshenko, Ye., Rustenbach, J., Aydogar, Oe., Berghofer, G., Lichtenegger, H., Delva, M., Schelch, G., Pirsich, K., Fremuth, G., Steller, M., Arnold, H., Raditsch, T., Auster, U., Fornaçon, K.-H., Schenk, H. J., Michaelis, H., Motschmann, U., Roatsch, T., Sauer, K., Schröter, R., Kurths, J., Lenners, D., Linthe, J., Kobzev, V., Styashkin, V., Achache, J., Slavin, J., Luhmann, J. G. and Russell, C. T. (1989) Magnetic fields near Mars: first results. *Nature* **341**, No. 6243, 604.
- Rosenbauer, H., Shutte, N., Apáthy, I., Galeev, A., Gringauz, K., Grünwaldt, H., Hemmerich, P., Jockers, K., Király, P., Kotova, G., Livi, S., Marsch, E., Richter, A., Riedler, W., Remizov, T., Schwenn, R., Schwingenschuh, K., Steller, M., Szegő, K., Verigin, M. and Witte, M. (1989) Ions of Martian origin and plasma sheet in the Martian magnetosphere: initial results of the Taus experiment. *Nature* **341**, No. 6243.

- Russell, C. T. (1977) On the relative locations of the bow shocks of the terrestrial planets. *Geophys. Res. Lett.* **4**, 387.
- Russell, C. T. (1978a) The magnetic field of Mars: Mars 3 evidence reexamined. *Geophys. Res. Lett.* **5**, 81.
- Russell, C. T. (1978b) The magnetic field of Mars: Mars 5 evidence reexamined. *Geophys. Res. Lett.* **5**, 85.
- Russell, C. T. (1985) Planetary bow shocks, in *Collisionless Shocks in the Heliosphere: Reviews of current Research*, pp. 109-130. Geophys. Monograph 35, AGU.
- Russell, C. T., Elphic, R. C. and Slavin, J. A. (1980) Limits on the possible intrinsic magnetic field of Venus. *J. geophys. Res.* **85**, 8319.
- Schwingschuh, K., Riedler, W., Lichtenegger, H., Yeroshenko, Ye., Sauer, K., Luhmann, J. G., Ong, M. and Russell, C. T. (1991) The Martian bow shock: Phobos observations. *Geophys. Res. Lett.* (in press).
- Spreiter, J. R. and Stahara, S. S. (1980) A new predictive model for determining solar wind-terrestrial planet interactions. *J. geophys. Res.* **85**, 6769.
- Vaisberg, O. and Smirnov, V. (1986) The Martian magnetotail. *Adv. Space Res.* **6**, 301.
- Whang, Y. C. (1977) Magnetospheric magnetic field of Mercury. *J. geophys. Res.* **82**, 1024.
- Yeroshenko, Ye., Riedler, W., Schwingschuh, K., Luhmann, J. G., Ong, M. and Russell, C. T. (1991) The magnetotail of Mars. *Geophys. Res. Lett.* (in press).